Application of Bone Collagen Matrix combined with HUC-MSCs for Alveolar Process Cleft in a Rabbit Model

Xue-Cheng Sun
Reproductive and Genetic Center of National Research Institute for Family Planning
https://orcid.org/0000-0002-1689-2627
Hu Wang
Reproductive and Genetic Center of National Research Institute for Family Planning
Dan Zhang
Reproductive and Genetic Center of National Research Institute for Family Planning
Jian-Hui Li
Reproductive and Genetic Center of National Research Institute for Family Planning
Li-Qiang Yin
Yantai Zhenghai Bio-Tech Co., Ltd.
Yu-Fang Yan
Yantai Zhenghai Bio-Tech Co,. Ltd.
Xu Ma (genetic@263.net.cn)
Reproductive and Genetic Center of National Research Institute for Family Planning
Hong-Fei Xia (hongfeixia@126.com)
Reproductive and Genetic Center of National Research Institute for Family Planning

Research Article

Keywords: Alveolar process cleft, Bone collagen matrix, Japanese white rabbits (JWRs), Human umbilical cord mesenchymal stem cells (HUC-MSCs), Micro-focus computerized tomography (micro-CT)

Posted Date: March 24th, 2021

DOI: https://doi.org/10.21203/rs.3.rs-335429/v1

Version of Record: A version of this preprint was published at Stem Cell Reviews and Reports on August 22nd, 2021. See the published version at https://doi.org/10.1007/s12015-021-10221-y.

Abstract

Background: Most materials used clinically for filling severe bone defects lack the ability to induce bone regeneration or low bone conversion rate, therefore, their therapeutic effects are limited. Human umbilical cord mesenchymal stem cells (HUC-MSCs) have good osteoinduction. The mechanism of heterogeneous bone collagen matrix combined with HUC-MSCs in repairing bone defects of alveolar process cleft is still unclear.

Methods: Here, a rabbit alveolar process cleft model was established to evaluate the repair effect and molecular mechanism of bone collagen matrix and its combination with HUC-MSCs on critical-sized bone defects in the alveolar process. We randomly divided 48 young Japanese white rabbits (JWRs) into normal, control, material and MSCs groups. The alveolar process cleft model was established by removing the bone of equal volume at the left maxillary. Bone collagen matrix combined with HUC-MSCs that were then implanted in the defect area. X-ray analysis and blood analysis were analyzed 3 months after surgery. Skull tissues were collected for micro-focus computerized tomography (micro-CT) analysis and histochemical staining. The above experiment was repeated 6 months after surgery.Results: the main findings

Results: It was found that bone collagen matrix and HUC-MSCs showed good biocompatibility. Heterogeneous bone collagen matrix combined with HUC-MSCs significantly enhanced osteoinduction and osteoconduction.

Conclusions: This experiment provides a new method for repairing alveolar process cleft.

Trial registration: Not applicable.

1. Introduction

Alveolar process cleft is common in clinic. Alveolar bone defects caused by birth defect trauma and inflammation seriously affect the patient's facial and oral functions. It also brings great difficulties to the patient's subsequent denture repair. The goal of alveolar bone reconstruction is to obtain bone with physiological function and eventually restore facial morphology and occlusal function. At present, autogenous bone transplantation is still the clinical gold standard, the common autogenous bone has skull [1], cancellous bone [2], ilium [3] and so on. In addition, there are dozens of bone substitutes, such as allogeneic bone [4], allogeneic bone [5] and tissue-engineered bone [6], that have been applied in clinical practice.

The ideal bone repair material needs to consider a number of factors. On the one hand, it should have a wide range of sources, high biocompatibility and safety. On the other hand, it must have certain plasticity and degradability. In addition, it also need to have good bone conductivity and bone inductance. The collagen matrix used in this study was made from bovine cancellous bone through a series of decellularization and degreasing processes. Its main ingredients are hydroxyapatite and collagen. The

material not only greatly reduced its immunogenicity, but also maintained the natural structure of the bone. The material has a suitable pore size to facilitate the growth of cells and blood vessels. The environment of bone regeneration is complex, so it is difficult to meet the need of bone regeneration simply using Bone collagen matrix. Studies have shown that HUC-MSCs play an important role in inducing bone regeneration [7-9]. HUC-MSCs have the advantages of wide availability, rapid proliferation and low immunogenicity [9]. Fetal umbilical cord belongs to medical waste, so the HUC-MSCs have low ethical controversy. Therefore, in this study, HUC-MSCs were inoculated into bone collagen matrix to induce bone regeneration and repair.

How to make a suitable animal model of alveolar bone defect according to the clinical characteristics of oral bone grafting surgery is the basis and focus of studying alveolar bone repair and evaluating the osteogenic ability of bone grafting materials. Many researchers have used monkey [10], beagle [11-12], miniature pig [13-14], rabbit [15], rat [16] and other experimental animals to make bone defect models in different parts of their jaws. After the implantation of bone material, the ability to reconstruct the jaw bone was assessed by pathological methods. Compared with other animals, rabbits have the advantages of short growth cycle, easy feeding and low cost. And the rabbit body size is moderate, gentle temperament, easier to operate. So many researchers have also used rabbits to make models of alveolar process cleft [17-19].

In this study, JWRs were selected as experimental animals based on our previous research [20], and part of their left maxilla was removed by surgery to prepare the alveolar process cleft model. Considering that rabbit has more blood supply sources and stronger self-healing ability than human, the bone defect should meet the CSD (critical size defect) [21]. This provides an important model basis for evaluating the osteogenic capacity of Bone collagen matrix after inoculation with HUC-MSCs.

2. Materials And Methods

2.1 Isolation and culture of HUC-MSCs

HUC-MSCs were isolated from Wharton’s jelly using tissue block adherent culture. First, the blood vessels of the human umbilical cord were removed, and then the cord was cut into about one cubic millimeter of tissue. The tissue block was attached to the bottom of the cell culture dish and cultured in a carbon dioxide incubator for 20 days. The primary cells were collected and then passed for culture. The HUC-MSCs used in this study were previously identified by our lab [22].

2.2 Preparation of implant materials

The bone collagen matrix is the heterogeneous bone matrix made from bovine cancellous bone after a series of processes, retaining its natural three-dimensional porous structure. The main ingredients are hydroxyapatite and collagen. The collagen membrane that covers the site of the injury after adding the Bone collagen matrix were derived from bovine skin. The thickness of the collagen membrane is about 0.8 mm. Before use, cut the collagen membrane into small pieces equal to the defect area. The Bone

collagen matrix and the collagen membrane were provided by zhenghai biotechnology co. LTD（Yantai, China）. HUC-MSCs (concentration : 10^7 cells/mL) within 5 generations were collected to be inoculated with bone collagen matrix and cultured in carbon dioxide incubator for 0.5 h.

2.3 Groups and treatment

In this study, we used 48 female JWRs (bodyweight: 2000±300 g). These JWRs were purchased from huafukang biotechnology co. LTD（Beijing, China）. All these animals were kept in the animal room of National Research Institute for Family Planning. Provide them with clean water and food. Indoor conditions are as follows: temperature (24±1℃), air humidity (55%±5%), noise (less than 60dB), lighting time (12 h). Keep the room clean, dry and ventilated at all times. The experiment was approved by the local research and ethics committee.

The study was designed to be divided into four groups, each of which was randomly assigned to twelve JWRs. They were normal, control, material and MSCs groups. Rabbits were anesthetized by intravenous injection of serazine hydrochloride into the ear margin (concentration: 1-2 mg/kg). Look for the left maxilla after the rabbit is anesthetized. The alveolar process cleft model was established by removing the equal volume of the jaw bone with the rongeur (Fig. 1).

The normal group was fed normally. In the control group, after removing part of jaw bone, collagen membrane was directly covered and the muscles and skin at the injured site were sutured. In the material group, after removing part of jaw bone, the bone collagen matrix of the same volume was filled, and then the collagen membrane was directly covered and the muscles and skin of the injured site were sutured. In the MSCs group, after removing part of jaw bone, the bone collagen matrix of the same volume composite HUC-MSCs was filled, and then the collagen membrane was directly covered and the muscles and skin of the injured site were sutured. Conventional anti-inflammatory therapy was given for 1 week to prevent postoperative infection. Three rabbits were taken from each group at 3 and 6 months postoperatively. All rabbits were euthanized, and the transplant site was examined. Fresh skull tissue was first fixed in 4% paraformaldehyde for 24h, then decalcified with 10% EDTA for 1 month, and finally embedded in paraffin. Paraffin sections (6 mm) were prepared by rotary microtome (Leica RM2245, Leica, Gmbh, Germany). For histology staining, paraffin *sectionswere deparaffinized* in xylene and rehydrated through graded alcohol solutions to water.

2.4 X-ray analysis

X-ray analysis was performed on the surgical sites of each group 3 and 6 months after surgery. We used a Softex M-60 x-ray machine (Kanagawa, Japan) at the Beijing ornamental animal hospital. The examination parameters were set as follows: 80 kV, 125 mA and an exposure time of 40 ms.

2.5 Blood analysis

Three rabbits were randomly selected from each group 3 months and 6 months after surgery. About 3.5ml of blood was collected by ear vein sampling, some of which were used for direct detection and the other for serum separation. Blood routine, liver function, renal function and serum bone gla protein (BGP) of rabbits were detected. Routine blood tests were performed using an LH 750 automated haematology analyser (Beckman Coulter, USA). The blood biochemistry test was performed using a DXC 800 automated biochemical analyser (Beckman Coulter, USA).

2.6 Micro CT analysis

Three rabbits were randomly selected from each group at 3 months and 6 months after surgery. It was euthanized and a skull model was made. The general appearance of the skull is recorded from lateral and vertical perspectives. The maxillary region of the skull was scanned by micro CT. Bone regeneration in each group was evaluated by micro CT. Bone regeneration in the *m*aterial transfer area was evaluated by a micro CT system (SIEMENS Inveon Research Workplace 4.2, Beijing). The repair of maxillary region in each group was observed from a stereoscopic perspective. The bone trabeculae and bone mineral density of bone regeneration area in each group were analyzed.

2.7 Hematoxylin and eosin (HE) staining

HE staining was used to observe tissue morphology. The nucleus is stained blue by hematoxylin and the other areas are colored red by eosin. TE2000-U inverted phase contrast microscope (Nikon, Tokyo, Japan) was used to observe bone histomorphological changes.

2.8 Periodic Acid-Schif (PAS) staining

PAS staining was used to assess the glycogen content. PAS staining was performed using a commercial kit (SenBeiJia Biological Technology Co. Ltd, NanJing, Jiangsu, China) *according to the manufacturer*'s *instructions*. Briefly, the sections were incubated with periodic acid solution in dark for 5 min, then incubated with the Schiff reagent in dark for 20 min at room temperature. The sections were counterstained with *Lillie-Mayer*'s *hematoxylin. The samples* were visualized by using differential interference contrast (DIC) optics microscopy (DM IL LED, Leica Gmbh, Germany).The structure of cartilage can be dyed deep purple or deep red.

2.9 Sirius redstaining

Sirius red staining was used to detected different collagen fibers. Sirius red staining was performed using a commercial kit (SenBeiJia Biological Technology Co. Ltd, NanJing, Jiangsu, China) *according to the manufacturer*'s *instructions*. Briefly, the sections were incubated with Sirius red for 1 h at room temperature, then counterstained with Mayer's *hematoxylin.* Sirius red can dye type 1 collagen bright orange. Image J software was used to calculate the relative percentage of type 1 collagen staining area under different fields in each group.

2.10 Bone-specific Alkaline Phosphatase (ALP) assay

Bone-specific ALP is one of the phenotypic markers of osteoblasts, which can directly reflect the activity or function of osteoblasts. Calcium-cobalt staining of alkaline phosphatase was used to detected the *bone*-specific ALP content by a commercial kit (KeyGEN BioTECH Co.Ltd, NanJing, Jiangsu, China) *according to the manufacturer*'s *instructions*. Briefly, the sections were incubated with ALP solution for 5 min, then incubated with Cobalt nitrate solution for 2 min at room temperature. The sections were counterstained with eosin. Osteoblasts can be dyed black.

2.11 Immunohistochemical staining for bone morphogenetic protein 2 (BMP-2) and Ki67

After dewaxing, hydration and heat-induced epitope retrieval, the sections were incubated with rabbit anti-BMP-2 polyclonal antibody (Immunoway, Plano, TX, USA Plano, TX, USA, 1:200) and mouse anti Ki-67 monoclonal antibody (Abcam, Cambridge, UK, 1:200) respectively, then incubated with HRP-conjugated goat anti-rabbit or mouse IgG (*Jackson Immunoresearch Laboratories*, West Grove, Pennsylvania, USA, 1:5000). The sections were developed with diaminobenzidine tetrahydrochloride (DAB) and counterstained with hematoxylin. Three fields were randomly selected for each section, and the percentage of Ki67 positive cells was calculated using Image J software.

2.12 Detection of apoptosis assay by TdT-mediated dUTP nick-end Labelling (TUNEL)

TUNEL was performed by using an in-situ Cell Death Detection Kit, Fluorescein (Roche, Mannheim, Germany) *according to the manufacturer*'s *instructions*. For the correlation of TUNEL with nuclear morphology, sections were counterstained with *Hoechst 33258*. Apoptotic cells were counted in 3 different optical fields (magnification ×400) selected in a random manner. Samples were viewed at excitation 488 nm/emission 512 nm by fluorescence microscopy (ZEISS LSM 510 META, Germany). At least 500 cells for each sample were evaluated for apoptosis in different optical fields (magnification ×400) randomly selected. The results were expressed as the ratio of TUNEL-positive cells to total cells. Each treatment was repeated at least three times.

2.13 Statistical analysis

The results are presented as mean ± SD and $P < 0.05$ was considered statistically significant. Data were analyzed statistically by One-way ANOVA and the Student's *t*-test with GraphPad Prism software (GraphPad Prism 6).

3. Results

3.1 Morphometric analysis of alveolar process tissues

General visual observation showed that the injury side was compared with the normal side in each group. At 3 months, no obvious repair was found in the bone defect area of the material group and the control group, while partial repair was found in the bone defect area of the MSCs group (Fig. 2A). At 6 months, there was no obvious repair in the bone defect area of the material group, partial repair in the bone defect area of the control group, and basic repair in the bone defect area of the MSCs group (Fig. 2B).

In order to evaluate bone repair of alveolar process cleft, X-ray was used for preliminary analysis (Fig. 3), in which bone density was positively correlated with brightness. Compared with the normal group, we found that the bone mineral density of the control group was the lowest, that of the MSCs group was the highest, and that of the material group was between the two groups at 3 months. At 6 months, the bone density of the MSCs group was still higher than that of the other groups. Therefore, we can infer that the osteogenic rate of bone collagen matrix combined with HUC-MSCs is significantly higher than the effect of bone collagen matrix alone.

In order to further analyze the absorption of bone materials and bone formation of alveolar process cleft, micro-CT scan was used to detect skull tissues from different perspectives at 3 and 6 months after surgery. The red box is the material transplantation area. The injury side was compared with the normal side in each group. The results of micro-CT scan were consistent with those of the General observation. A significant amount of new bone tissue was found on the injury side of the MSCs group 6 months after surgery (Fig. 4B). We calculated the percentage of bone density and the percentage of trabecular bone in each group (Fig. 4C). At 3 months after surgery (Fig. 4Ca), the results showed that the percentage of trabecular bone in MSCs group (60.916 ± 2.072 %) was the highest, followed by the material group (52.647 ± 2.857 %) and the control group was 0. The results at 6 months (Fig. 4Cc) were similar to those at 3 months (MSCs group: 73.338 ± 2.132 %, material group: 61.180 ± 4.241 %, control group: 0). The results showed that the percentage of bone density in control group (0.466 ± 0.110 %) was the lowest, the material (53.013 ± 2.002 %) and MSCs groups (64.337 ± 2.011 %) was not significantly different at 3 months after surgery (Fig. 4Cb). The percentage of bone density in MSCs group (82.936 ± 2.112 %) was significantly higher than that of the other two groups (material group: 43.858 ± 0.522 %, control group: 1.29 ± 0.522 %) at 6 months after surgery (Fig. 4Cd). Therefore, the osteogenic ability of bone collagen matrix combined with HUC-MSCs was significantly better than that of bone collagen matrix alone.

3.2 Microscopic structure of bone defect site detected by HE staining

HE staining showed that no significant bone repair was observed in the control group in both periods (Fig. 5 Aa1 & Ae1). 3 months after the surgery, a few bone fibers, bone marrow, bone trabeculae and a large number of cavitation structures were observed in the damaged area of the material group (Fig. 5 Ac1). At 6 months after the surgery, trabecular bone, bone marrow and cavitation structures were observed in a small number of bone repair areas in the material group (Fig. 5 Ag1). In the MSCs group, no cavitation was observed in the damaged area at 3 months after surgery, and a large number of bone trabeculae and fibrous tissues were observed (Fig. 5 Ad1). At 6 months after the surgery, bone trabeculae in the damaged area of the MSCs group had been connected to form bone tissue (Fig. 5 Ah1). The results of HE staining indicated that MSCs group had a better repair effect.

3.3 Measurement of serum Bone gla protein (BGP)

BGP is a *bone*-specific *protein*. It is synthesized by the osteoblast and incorporated into the *bone* matrix. Serum BGP results showed that the BGP content of the control group and the material group was close to that of the normal group, while that of the MSCs group was significantly higher than that of the normal

group (Fig. 5 B1 & B2). The results showed that the osteogenic ability of bone collagen matrix combined with HUC-MSCs was significantly better than that of bone collagen matrix alone.

3.4The effect of bone collagen matrix combined with hUC-MSCs on osteoblasts, collagen and saccharides associated with bone formation

ALP staining was used to detected the osteoblasts that were stained black color. The results of ALP staining showed that the normal maxillary was a uniform bone matrix without osteoblasts (Fig. 6 a & e). By comparing the results of PAS staining in the two periods, we found that there were no obvious black areas in the control group (Fig. 6 b & f). In the material group, black appeared on the edge of the bone trabecular at 3 months after surgery (Fig. 6 c), and no black area was observed at 6 months after surgery (Fig. 6 g). In the MSCs group, black appeared at the edge of the bone trabecular at 3 months after surgery (Fig. 6 d), and remained at 6 months after surgery (Fig. 6 h). The results showed that bone collagen matrix combined with HUC-MSCs could promote osteoblasts better than bone collagen matrix alone.

Sirius red staining was used to analyze the collagen distribution. Sirius red can dye type 1 collagen into bright orange. The Sirius red stain showed the uniform distribution of type 1 collagen in the normal maxillary (Fig. 7 Aa & Ae). In the control group, only a very small amount of type 1 collagen was present (Fig. 7 Ab & Af). In the material group, a small amount of collagen type 1 was observed in the bone defect area after the implantation of bone collagen matrix alone (Fig. 7 Ac & Ag). However, after the implantation of bone collagen matrix combined with HUC-MSCs, a large amount of collagen type 1 was observed in the bone defect area (Fig. 7 Ad & Ah). The statistical results showed that the content of collagen type 1 in the MSCs group was similar to that in the normal group (Fig. 7 B & C). The content of type 1 collagen in the control group and the material group was significantly lower than that in the normal group. The results showed that bone collagen matrix combined with HUC-MSCs could induce type 1 collagen more effectively than bone collagen matrix alone.

PAS staining was used to assay the saccharide content. The saccharide is a constituent part of matrix of cartilage. The results of PAS staining showed that the normal maxillary was a uniform bone matrix without chondrocytes (Fig. 8 a & e). By comparing the results of PAS staining in the two periods, we found that there were no obvious red or fuchsia areas in the control group (Fig. 8 b & f). At 3 months after the surgery, the bone trabecular border of the material group appeared red or fuchsia (Fig. 8 c), which was significantly reduced at 6 months after the surgery (Fig. 8 g). At 3 months after the surgery, the bone trabecular of the MSCs group showed large areas of fuchsia (Fig. 8 d), while at 6 months only the edges of the new bone tissue showed fuchsia (Fig. 8 h). The results showed that bone collagen matrix combined with HUC-MSCs could promote chondrocytes better than bone collagen matrix alone.

3.5The effect of bone collagen matrix combined with hUC-MSCs on BMP-2

The expression of BMP-2 in tissues is detected by immunochemistry. Since there was no obvious bone repair in the control group, BMP-2 expression was not observed in the two periods (Fig. 9 b & f). In the material group, BMP-2 was mainly concentrated in osteocytes and osteoclasts at the edge of the bone

trabecular (Fig. 9 c & g). In the MSCs group, BMP-2 was mainly expressed at the edge of bone trabecular at 3 months after surgery (Fig. 9 d), and at 6 months after surgery, BMP-2 was mainly expressed in the growth area of new bone tissue (Fig. 9 h). The results showed that the ability of bone collagen matrix combined with HUC-MSCs to induce BMP-2 generation was better than that of bone collagen matrix alone.

3.6 Proliferation and apoptosis analysis of bone defect site detected

TUNEL assay was used to detect apoptosis in the bone defect center of each group, and the apoptotic nuclei were stained brown (Fig. 10 A). Ki67 immunohistochemistry was used to detect the proliferation of cells in the bone defect center of each group, and the proliferation cells were labeled with green fluorescence (Fig. 10 B). Since no bone tissue was formed in the bone defect center of the control group and the material group, the cell proliferation rate and apoptosis rate were statistically 0. TUNEL results showed that the apoptosis rate of the MSCs group was significantly higher than that of the normal group at 3 months after surgery. The apoptosis rate at 6 months after surgery was significantly lower than that of the normal group (Figure 10 C1). The immunohistochemical results of Ki67 showed that the proliferation rate of the MSCs group was close to that of the normal group in both periods (Figure 10 C2). The proliferating cells of MSCs group were mainly concentrated in the bone growth area (Figure 10Bh1). Therefore, bone collagen matrix combined with HUC-MSCs can effectively promote bone regeneration and repair by regulating cell proliferation and apoptosis.

3.7 Assessment of postoperative health status of rabbits

Blood routine (Table 1& Table 4), liver function (Table 2 & Table 5) and renal function (Table 3 & Table 6) were used to estimate health status of rabbits at 3 and 6 months after the surgery. Then the values of each group were compared with those of the normal group and the control group. Blood routine results showed that lymphocyte (LYM) content decreased and neutrophil granulocyte (NEUT) content increased in the MSCs group at 3 months, and returned to normal at 6 months. C-reactive protein (CRP) content in the material group was higher than that in the normal group at 3 and 6 months, but the value decreased. CRP content in the control group was higher than that in the normal group at 3 months and close to that in the normal group at 6 months. It was suggested that the control group and MSCs group had mild inflammatory response at 3 months and tended to be normal at 6 months. The material group remained in a state of mild inflammation. Liver function results showed mildly abnormal aspartate aminotransferase (AST) and alanine aminotransferase (ALT) values in the material group at 3 months and normal values at 6 months. This suggests that the control group had a mild inflammatory response at 3 months and tended to be normal at 6 months. ALP content in the control, material and the MSCs groups was higher than that in the normal group at 3 months and lower than that in the normal group at 6 months. This suggests that osteoblasts increase substantially at 3 months and become normal at 6 months. Renal function results showed that CR was higher in the control group and the material group, and blood urea nitrogen (BUN) and creatinine (CR) were higher in the MSCs group at 3 months. All indicators were normal at 6 months. To sum up, compared with the normal group, the control group, the

material group and the MSCs group all had mild inflammatory responses at 3 months. At 6 months, all the indicators in each group were basically normal. CRP in the material group was relatively high at 6 months, compared with that in the MSCs group, adding HUC-MSCs reduced the inflammatory response.

4. Discussion

Bone induction refers to the induction of connective tissue adjacent to the bone graft area by bone growth factors or seed cells in the bone material. By affecting undifferentiated bone progenitor cells, promoting their differentiation and proliferation and eventually becoming osteoblasts, the formation of new bone is facilitated.

In recent years, MSCs have been widely used in the treatment of various organ and tissue injuries [23-25]. In vivo experiments have confirmed that HUC-MSCs can repair vascular and tissue epithelial injury [26]. Studies have also found that HUC-MSCs play an important role in inducing bone regeneration [7-9]. HUC-MSCs are characterized by easy extraction, multidirectional differentiation, short proliferation time, low immunogenicity, and long survival time after transplantation, have become the preferred seed cells for transplantation[27-28].HUC-MSCs were obtained from neonatal umbilical cords. Neonatal umbilical cords are clinical waste, so there are few ethical implications [29]. The obtained stem cells showed rapid self-renewal [30]. HUC-MSCs also express low levels of major histocompatibility complex II and costimulatory molecules, thereby reducing rejection [31]. HUC-MSCs are easy to be absorbed and degraded in vivo, so appropriate scaffold materials are needed to play a better role. Collagen scaffolds is an ideal scaffold material to enhance the action of HUC-MSCs on bone defect sites [8].

The bone collagen matrix used in this study is bone matrix made from bovine cancellous bone after degreasing and decellularization process. After decalcification and deproteinization, the heterogeneous bone matrix is mainly composed of type 1 collagen, which is insoluble and highly hinged. The heterogeneous bone matrix has good bone-guiding activity, toughness and strength. The material preserves the natural structure of the bone and has the right pore size for cells and blood vessels to grow in. Due to the removal of antigens, the antigenicity of the material is very weak, and the rejection after implantation is not obvious. The heterogeneous bone matrix is more widely derived than the allogeneic bone, and can be degraded and absorbed in a shorter time, all of which meet the requirements of ideal carrier.

Studies have shown that the function of collagen biomaterials alone no obvious effective in bone repair [32]. The combination of bone collagen matrix can slowdown the degradation rate of HUC-MSCs, thus prolonging the bone repair time.

Therefore, we believe that HUC-MSCs combined with bone collagen matrix has obvious osteogenic induction ability. The joint transplantation of both contributed to the repair of maxillary injury and restoration of occlusal function, likely through promote the expression of osteoblasts, chondrocytes, type 1 collagen and BMP-2. The results of blood analysis suggested that HUC-MSCs could reduce inflammatory response. Studies have suggested that HUC-MSCs may play a repair role by inhibiting

inflammation [22]. Therefore, its application to the human body caused by the inflammatory response needs further research.

5. Conclusions

With the development of tissue engineering methods, the HUC-MSCs combined with collagen materials is a promising strategy for bone repair. The method of HUC-MSCs combined with bone collagen matrix to fill l a bone defect site is simple, rapid and suitable for the defective maxilla. This study shows that the combination of HUC-MSCs with bone collagen matrix is a promising strategy in the field of regenerative medicine and bone repair.

Abbreviations

Japanese white rabbits (JWRs)

Human umbilical cord mesenchymal stem cells (HUC-MSCs)

Micro focus computerized tomography (micro CT)

Hematoxylin eosin (HE)

Alkaline phosphatase (ALP)

Periodic Acid-Schiff stain (PAS)

Immunohistochemical (IHC)

TdT-mediated dUTP nick-end Labelling (TUNEL)

Bone gla protein (BGP)

Declarations

Acknowledgements

The authors are very grateful to the National Key Research and Development Program of China We are also very grateful to the animal experiment center of the National Research Institute for Family Planning for its meticulous care of animals.

Funding

This work was funded by grants from the National Key Research and Development Program of China (2016YFC1000803).

Availability of data and materials

Bone Collagen Matrix and collagen membranes were provided by Zhenghai biotechnology co. LTD (Yantai, China)

Human umbilical cord were provided by Haidian Maternal & Child Health Hospital (Beijing, China)

Authors' contributions

XCS, XM and HFX designed the study. XCS, HW and JHL were responsible for the vivo surgery and performing the procedure. YFY and LQY provided the bone repair materials. HW and DZ were responsible for in vitro experiments. XCS, HW and HFX prepared the manuscript. XCS, HW, DZ and HFX were responsible for revising the manuscript critically for important intellectual content. All authors read and approved the final manuscript.

Ethical Approval

Ethical approval to report this case was obtained from the National Research Institute for Family Planning (Ethics Number 2015-16).

Consent for publication

Not applicable.

Competing interests

The authors declare that they have no competing interests.

Publisher's Note

Springer Nature remains neutral with regard to jurisdictional claims in published maps and institutional affiliations.

Authors' details

a Reproductive and Genetic Center of National Research Institute for Family Planning, Beijing, 100081, China

b Graduate Schools, Peking Union Medical College, Beijing, 100730, China

c Yantai Zhenghai Bio-Tech Co., Ltd. Shandong, 264006, China

Statement of Informed Consent

There are no human subjects in this article and informed consent is not applicable.

Statement of Human and Animal Rights

All procedures in this study were conducted in accordance with the National Research Institute for Family Planning (Ethics Number 2015-16) approved protocols.

References

[1] Cohen M, Figueroa A A, Haviv Y, et al. Iliac Versus Cranial Bone for Secondary Grafting of Residual Alveolar Clefts [J]. Plastic & Reconstructive Surgery, 1991, 87(3):423.

[2] Tai C C E, Sutherland I S, Mcfadden L. Prospective analysis of secondary alveolar bone grafting using computed tomography [J]. Journal of Oral & Maxillofacial Surgery Official Journal of the American Association of Oral & Maxillofacial Surgeons, 2000, 58(11):1241-1249.

[3] Larossa D, Buchman S, Rothkopf D M, et al. A Comparison of Iliac and Cranial Bone in Secondary Grafting of Alveolar Clefts [J]. Plastic and Reconstructive Surgery, 1995, 96(4):798-799.

[4] Rosenthal RK, Folkman J, Glowacki J, Demineralized bone implants for nonunion fracture, bone cysts, and fibous lesins [J]. Clinical Orthopaedics & Related Research, 1999, 364:61-69.

[5] Al-AsfourA, Farzad P, Andersson L, et al. Host tissue reactions of non-demineralized autogenic and xenogenic dentin blocks implanted in a non-osteogenic environment. An experimental study in rabbits [J]. Dental Traumatology, 2014, 30(3):198-203.

[6] Smith B T , Santoro M , Grosfeld E C , et al. Incorporation Of Fast Dissolving Glucose Porogens Into An Injectable Calcium Phosphate Cement For Bone Tissue Engineering [J]. Acta Biomaterialia, 2017, 50:68-77.

[7] Liu S, Hou KD, Yuan M et al. Characteristics of mesenchymal stem cells derived from Wharton's jelly of human umbilical cord and for fabrication of non-scaffold tissue-engineered cartilage [J]. Journal of Bioscience & Bioengineering, 2014, 117(2):229-235.

[8] Tassi S A, Sergio N Z, Misawa M Y O, et al. Efficacy of stem cells on periodontal regeneration: Systematic review of pre-clinical studies [J]. Journal of Periodontal Research, 2017, 52(5):793-812.

[9] Jin YZ, Lee JH. Mesenchymal stem cell therapy for bone regeneration [J]. Clinics in orthopedic surgery, 2018, 10(3):271–278.

[10] Hämmerle, CHF, Chiantella G, Karring T , et al. The effect of a deproteinized bovine bone mineral on bone regeneration around titanium dental implants [J]. Clinical Oral Implants Research, 1998, 9(3):151-162.

[11] Zoran Tatić, Novak Stamatović, Bubalo M, et al. Histopathological evaluation of bone regeneration using human resorbable demineralized membrane [J]. Vojnosanitetski pregled. Military-medical and pharmaceutical review, 2010, 67(6):480-486.

[12] Lee JS, Wike sjö UM, Jung UW, et al. Periodontal wound healing/ regeneration following implantation of recombinant human growth/ differentiation factor- 5 in a beta- tricalcium phosphate carrier into one-wall intrabony defects in dogs [J]. Journal of Clinical Periodontology, 2010, 37(4): 382- 389.

[13] Ruehe B, Niehues S, Heberer S, et al. Miniature pigs as an animal model for implant research: bone regeneration in critical-size defects [J]. Oral Surgery Oral Medicine Oral Pathology Oral Radiology & Endodontics, 2009, 108(5):699-706.

[14] Liu Y, Zheng Y, Ding G, et al. Periodontal Ligament Stem Cell-Mediated Treatment for Periodontitis in Miniature Swine [J]. Stem Cells, 2008, 26(4):1065-1073.

[15] Schmitz JP, Hollinger JO. The critical size defect as an experimental model for craniomandibulofacial nonunions [J]. Clinical Orthopaedics & Related Research, 1986, (205): 299- 308

[16] Gallego L, Junquera L, Garcia E, et al. Repair of rat mandibular bone defects by alveolar osteoblasts in a novelplasma- derived albumin scaffold [J]. Tissue Engineering Part A, 2010 16(4): 1179- 1187

[17] Puumanen K, M. Kellomäki, V. Ritsilä, et al. A novel bioabsorbable composite membrane of Polyactive 70/30 and bioactive glass number 13-93 in repair of experimental maxillary alveolar cleft defects [J]. Journal of Biomedical Materials Research Part B Applied Biomaterials, 2010, 75B(1):25-33.

[18] Kamal M, Andersson L, Tolba R, et al. A rabbit model for experimental alveolar cleft grafting [J]. Journal of Translational Medicine, 2017, 15(1).

[19] Djasim U M, Hekking-Weijma J M, Wolvius E B, et al. Rabbits as a model for research into craniofacial distraction osteogenesis [J]. British Journal of Oral & Maxillofacial Surgery, 2008, 46(8):620-624.

[20] Xue-Cheng Sun, Ze-Biao Zhang et al. Comparison of three surgical models of bone tissue defects in cleft palate in rabbits [J]. International Journal of Pediatric Otorhinolaryngology. 2019, (124):164-172.

[21] Schmitz J P, Hollinger J O. The critical size defect as an experimental model for craniomandibulofacial nonunions [J]. Clinical Orthopaedics & Related Research, 1986, 205(205): 299-308.

[22] Zhang L, Li Y, Guan C Y, et al. Therapeutic effect of human umbilical cord-derived mesenchymal stem cells on injured rat endometrium during its chronic phase [J]. Stem Cell Research & Therapy, 2018, 9(1):36.

[23] Mesenchymal stem cells -A new hope for radiotherapy-induced tissue damage [J]. Cancer Letters, 2015, 366(2):133-140.

[24] Petrella F, Rizzo S, Borri A, Casiraghi M, Spaggiari L. Current Perspectives in Mesenchymal Stromal Cell Therapies for Airway Tissue Defects [J]. Stem cells international, 2015.

[25] Trohatou O, Roubelakis MG. Mesenchymal stem/stromal cells in regenerative medicine: past, present, and future [J].Cell Reprograming. 2017, 19(4):217.

[26] Xu Y, Meng H, Li C, et al. Umbilical cord-derived mesenchymal stem cells isolated by a novel explantation technique can differentiate into functional endothelial cells and promote revascularization [J]. Stem Cells & Development, 2010, 19(10):1511.

[27] Cao FJ, Feng SQ. Human umbilical cord mesenchymal stem cells and the treatment of spinal cord injury. Chin Med J (Engl). 2009, 122(2):225–231.

[28] Baksh D, Yao R, Tuan RS. Comparison of proliferative and multilineage differentiation potential of human mesenchymal stem cells derived from umbilical cord and bone marrow [J]. Stem Cells. 2007, 25(6):1384–92.

[29] Wang Limin, Tran I, Seshareddy K, et al. A comparison of human bone marrow-derived mesenchymal stem cells and human umbilical cord-derived mesenchymal stromal cells for cartilage tissue engineering [J]. Tissue Eng A, 2009,15(8):2259-2266.

[30] Ding D C, Chang Y H, Shyu W C, et al. Human umbilical cord mesenchymal stem cells: a new era for stem cell therapy [J]. Cell Transplantation, 2015, 24(3):1515-1527.

[31] De Miguel, M. P. et al. Immunosuppressive properties of mesenchymal stem cells: advances and applications [J]. Current Molecular Medicine, 2012, 12(5): 574-591.

[32] Hollinger J O, Schmitt J M, Buck D C, et al. Recombinant human bone morphogenetic protein-2 and collagen for bone regeneration [J]. Journal of Biomedical Materials Research, 2015, 43(4):356-364.

Tables

Table 1 Blood routine test results 3 months after surgery.

Detection index	Unit	Normal group	Control group	Material group	MSCs group
RBC	10^{12}/L	5.460 ± 0.128	5.460 ± 0.831	5.823 ± 0.888	4.423 ± 0.839
HCT	%	35.400 ± 0.852	36.933 ± 3.260	36.500 ± 5.335	26.767 ± 6.956
RDW-CV	10^9/L	13.000 ± 0.883	12.400 ± 1.122	14.133 ± 1.893	13.767 ± 1.517
RDW-SD	%	29.567 ± 2.089	29.933 ± 2.590	31.300 ± 2.780	34.267 ± 3.430
MCV	fL	64.833 ± 0.125	68.300 ± 4.607	62.867 ± 3.967	68.800 ± 1.042
HBG	g/L	116.333 ± 5.249	120.000 ± 13.736	117.333 ± 15.413	98.333 ± 20.072
MCH	pg	21.233 ± 0.492	22.100 ± 0.883	20.300 ± 1.499	22.267 ± 0.759
MCHC	g/L	327.667 ± 7.760	324.333 ± 9.031	322.333 ± 6.018	323.667 ± 11.728
WBC	10^9/L	12.417 ± 3.685	8.655 ± 0.845	9.860 ± 1.520	7.150 ± 0.260
LYM#	10^9/L	4.438 ± 0.978	2.682 ± 0.664	2.449 ± 1.107	2.286 ± 0.702
LYM%	%	36.663 ± 3.101	37.443 ± 1.827	35.227 ± 3.915	23.440 ± 2.310**##
NEUT#	10^9/L	5.462 ± 1.451	4.993 ± 0.642	5.598 ± 0.738	4.654 ± 0.096
NEUT%	%	55.833 ± 4.129	54.537 ± 4.425	55.047 ± 2.917	66.140 ± 1.662*#
MONO#	10^9/L	0.655 ± 0.145	0.335 ± 0.027	0.694 ± 0.183	0.533 ± 0.104
MONO %	%	5.463 ± 0.902	4.997 ± 1.387	6.340 ± 1.085	7.840 ± 1.146
EO#	10^9/L	0.209 ± 0.047	0.161 ± 0.034	0.260 ± 0.193	0.246 ± 0.151
EO %	%	1.747 ± 0.289	2.563 ± 1.269	3.210 ± 1.010	2.237 ± 0.439
BASO	10^9/L	0.033 ± 0.008	0.033 ± 0.018	0.013 ± 0.008	0.028 ± 0.009
BASO %	%	0.293 ± 0.103	0.460 ± 0.123	0.177 ± 0.076	0.343 ± 0.174
PLT	10^9/L	155.333 ± 35.113	152.000 ± 17.682	123.333 ± 7.587	158.333 ± 32.602
PDW	%	16.100 ± 0.294	16.333 ± 0.419	15.633 ± 0.450	16.433 ± 0.660
MPV	fL	7.500 ± 0.283	7.600 ± 0.638	6.967 ± 0.262	7.200 ± 0.141
PLCR	%	17.000 ± 3.001	16.333 ± 2.530	11.600 ± 0.779	16.000 ± 3.024
PCT	%	0.043 ± 0.021	0.037 ± 0.005	0.018 ± 0.002	0.025 ± 0.011
CRP	mg/L	6.567 ± 1.195	11.75 ± 8. 380	16.465 ± 1.565	3.850 ± 0.650

Mean SD values were calculated for each group. * represents the statistical difference between each group and the normal group. # represents the statistical difference between each group and the control group.*, # P<0.05; **, ## P<0.01. RBC: red blood cell; HCT: hematocrit; RDW-CV: red blood cell volume distribution width; RDW-SD: red blood cell distribution width ; MCV: mean corpuscular volume ; HBG: hemoglobin; MCH: mean corpuscular hemoglobin; MCHC: mean corpuscular hemoglobin concentration; WBC: white blood cell; LYM: lymphocyte ;NEUT: neutrophile granulocyte; MONO: monocyte; EO: eosinophil; BASO: basophil; PLT: platelet; PDW: platelet distribution width; MPV: mean platelet volume; PLCR: platelet-large cell ratio; PCT: procalcitonin; CRP: C reactive protein.

Table 2 Liver function test results in blood at 3 months postoperatively.

Detection index	Unit	Normal group	Control group	Material group	MSCs group
ALT	IU/L	45. 267 ± 5.016	39. 400 ± 10.500	73. 267 ± 21.770	35.350 ± 0.650
AST	IU/L	30. 500 ± 6.309	17. 200 ± 0.100	43. 567 ± 11.912	25.050 ± 3.250
ALP	IU/L	38. 600 ± 2.900	45. 433 ± 6.585	66. 567 ± 14.946	56.000 ± 27.050
TP	g/L	53. 533 ± 0.903	54. 733 ± 2.522	54. 367 ± 5.672	56.767 ± 2.549
ALB	g/L	31. 633 ± 2.216	34. 700 ± 2.471	34. 833 ± 5.226	35.467 ± 0.309
GLB	g/L	21. 867 ± 3.081	20. 067 ± 1.967	19. 500 ± 0.698	21.300 ± 2.273
A/G		1. 487 ± 0.282	1. 753 ± 0.257	1. 783 ± 0.237	1.680 ± 0.159
TBIL	Umol/L	9. 363 ± 1.095	7. 280 ± 1.417	6. 370 ± 1.410	11.030 ± 1.015#
DBIL	Umol/L	5. 460 ± 0.235#	3. 380 ± 0.511*	3. 523 ± 0.288*	5.533 ± 0.903#
IBIL	Umol/L	4. 650 ± 0.170	5. 260 ± 0.050	3. 785 ± 0.085*##	5.497 ± 0.284*

Mean SD values were calculated for each group. * represents the statistical difference between each group and the normal group. # represents the statistical difference between each group and the control group.*, # P<0.05; **, ## P<0.01. ALT: alanine aminotransferase; AST: aspartate aminotransferase; ALP: alkaline phosphatase; TP: total protein; ALB: albumin; GLB: globulin; TBIL: total bilirubin; DBIL: bilirubin direct; IBIL: indirect bilirubin.

Table 3 Renal function results test in blood at 3 months postoperatively.

Detection index	Unit	Normal group	Control group	Material group	MSCs group
BUN	mmol/L	7.277 ± 1.950	8.193 ± 1.576	9.697 ± 1.101	12.323 ± 2.768
CR	mmol/L	65.210 ± 6.462	102.250 ± 16.693	95.040 ± 3.693	88.985 ± 5.195
UA	mmol/L	31.467 ± 2.155	29.700 ± 0.000	29.800 ± 1.675	29.700 ± 0.000

Mean SD values were calculated for each group. * represents the statistical difference between each group and the normal group. # represents the statistical difference between each group and the control group.*, # P<0.05; **, ## P<0.01. BUN: blood urea nitrogen; CR: creatinine; UA: uric acid.

Table 4 Blood routine test results at 6 months postoperatively.

Detection index	Unit	Normal group	Control group	Material group	MSCs group
RBC	10^{12}/L	5.343 ± 0.191	5.443 ± 0.443	5.583 ± 0.961	5.040 ± 0.184
HCT	%	35.567 ± 1.281	38.467 ± 2.131	37.567 ± 5.236	32.633 ± 1.312
RDW-CV	10^9/L	12.800 ± 0.455	12.733 ± 0.403	13.167 ± 0.450	13.167 ± 0.094
RDW-SD	%	30.367 ± 2.660	32.233 ± 0.939	31.733 ± 1.247	30.567 ± 0.450
MCV	fL	66.667 ± 3.206	70.900 ± 2.670	67.700 ± 3.395	64.833 ± 0.544
HBG	g/L	122.000 ± 1.633	126.000 ± 7.483	122.667 ± 14.727	112.000 ± 2.160
MCH	pg	22.833 ± 0.694	23.033 ± 0.531	22.233 ± 1.576	22.267 ± 0.613
MCHC	g/L	343.000 ± 8.602	327.000 ± 11.045	327.333 ± 7.542	343.667 ± 9.741
WBC	10^9/L	12.057 ± 2.159	9.420 ± 0.243	15.217 ± 4.687	9.050 ± 1.040
LYM#	10^9/L	4.317 ± 0.868	3.157 ± 0.377	4.079 ± 0.942	2.920 ± 0.057
LYM%	%	35.680 ± 0.724	33.453 ± 3.371	27.387 ± 2.349*	32.600 ± 3.167
NEUT#	10^9/L	6.865 ± 1.266	5.553 ± 0.137	7.462 ± 0.064	5.380 ± 0.910
NEUT%	%	56.893 ± 0.696	58.997 ± 2.200	64.077 ± 2.309*	59.083 ± 3.129
MONO#	10^9/L	0.559 ± 0.023	0.507 ± 0.069	0.699 ± 0.072	0.460 ± 0.029
MONO %	%	4.777 ± 0.793	5.400 ± 0.861	5.973 ± 0.385	5.090 ± 0.332
EO#	10^9/L	0.290 ± 0.092	0.167 ± 0.039	0.305 ± 0.092	0.280 ± 0.071
EO %	%	2.443 ± 0.860	1.773 ± 0.424	2.023 ± 0.347	3.020 ± 0.399
BASO	10^9/L	0.025 ± 0.007	0.035 ± 0.002	0.078 ± 0.010**##	0.020 ± 0.008
BASO %	%	0.207 ± 0.066	0.377 ± 0.025	0.540 ± 0.086**	0.207 ± 0.090
PLT	10^9/L	142.000 ± 18.184	142.000 ± 12.083	165.333 ± 36.335	148.000 ± 13.441
PDW	%	15.767 ± 0.125	16.300 ± 0.424	16.000 ± 0.294	16.200 ± 0.163
MPV	fL	7.000 ± 0.216	7.167 ± 0.262	6.967 ± 0.125	6.933 ± 0.386
PLCR	%	12.700 ± 0.648	15.000 ± 1.651	14.200 ± 1.633	14.600 ± 3.395
PCT	%	0.027 ± 0.012	0.030 ± 0.008	0.050 ± 0.024	0.027 ± 0.009
CRP	mg/L	3.863 ± 1.707	2.960 ± 0.536	9.920 ± 1.598	3.367 ± 0.838

Mean SD values were calculated for each group. * represents the statistical difference between each group and the normal group. # represents the statistical difference between each group and the control group.*, # P<0.05; **, ## P<0.01. RBC red blood cell; HCT: hematocrit; RDW-CV: red blood cell volume distribution width; RDW-SD: red blood cell distribution width; MCV: mean corpuscular volume; HBG: hemoglobin; MCH: mean corpuscular hemoglobin; MCHC: mean corpuscular hemoglobin concentration;

WBC: white blood cell; LYM: lymphocyte; NEUT: neutrophile granulocyte; MONO: monocyte; EO: eosinophil; BASO: basophil; PLT: platelet; PDW: platelet distribution width; MPV: mean platelet volume; PLCR: platelet-large cell ratio; PCT: platelet volume; CRP: C reactive protein.

Table 5 Liver function test results in blood at 6 months postoperatively.

Detection index	Unit	Normal group	Control group	Material group	MSCs group
ALT	IU/L	61.533±17.310	52.133±15.964	37.300±5.679	55.200±9.335
AST	IU/L	22.400±1.657	17.000±1.800	21.000±4.537	28.150±0.650#
ALP	IU/L	67.433±2.007#	44.300±3.226*	38.800±9.200*	44.150±6.450*
TP	g/L	60.000±3.289	59.133±1.434	58.633±7.013	57.133±1.537
ALB	g/L	38.700±1.424	39.633±0.826	34.133±7.643	38.100±0.589
GLB	g/L	21.267±1.837	19.500±0.927	24.533±3.991	19.033±0.967
A/G		1.827±0.096	2.043±0.094	1.457±0.520	2.007±0.069
TBIL	Umol/L	5.027±0.659	5.073±1.377	5.573±1.311	4.647±0.898
DBIL	Umol/L	2.350±0.530	3.093±0.972	2.813±0.821	2.913±0.652
IBIL	Umol/L	2.677±0.885	1.980±0.743	2.325±0.405	1.990±0.140

Mean SD values were calculated for each group. * represents the statistical difference between each group and the normal group. # represents the statistical difference between each group and the control group.*, # $P<0.05$; **, ## $P<0.01$. ALT: alanine aminotransferase; AST: aspartate aminotransferase; ALP: alkaline phosphatase; TP: total protein; ALB: albumin; GLB: globulin; TBIL: total bilirubin; DBIL: bilirubin direct; IBIL: indirect bilirubin.

Table 6 Renal function results test in blood at 6 months postoperatively.

Detection index	Unit	Normal group	Control group	Material group	MSCs group
BUN	mmol/L	8.453±0.097	7.730±1.744	7.970±1.032	9.510±0.328
CR	mmol/L	90.983±5.695	108.427±11.757	96.057±21.218	107.480±5.195
UA	mmol/L	30.967±0.694	29.467±0.205	30.467±0.818	29.700±1.023

Mean SD values were calculated for each group. * represents the statistical difference between each group and the normal group. # represents the statistical difference between each group and the control group.*, # $P<0.05$; **, ## $P<0.01$. BUN: blood urea nitrogen; CR: creatinine; UA: uric acid.

Figures

Figure 1

A activated collagen matrix ; B the collagen membrane; C surgical process: a normal rabbit b The collagen membrane was trimmed and the bone collagen matrix was inoculated with HUC-MSCs. c the rabbit after anesthesia. d open the oral cavity after anesthesia. e-f remove the maxillary bone of equal volume. g measure the size of the bone that has been removed. h add materials i add collagen membrane. j suture the skin.

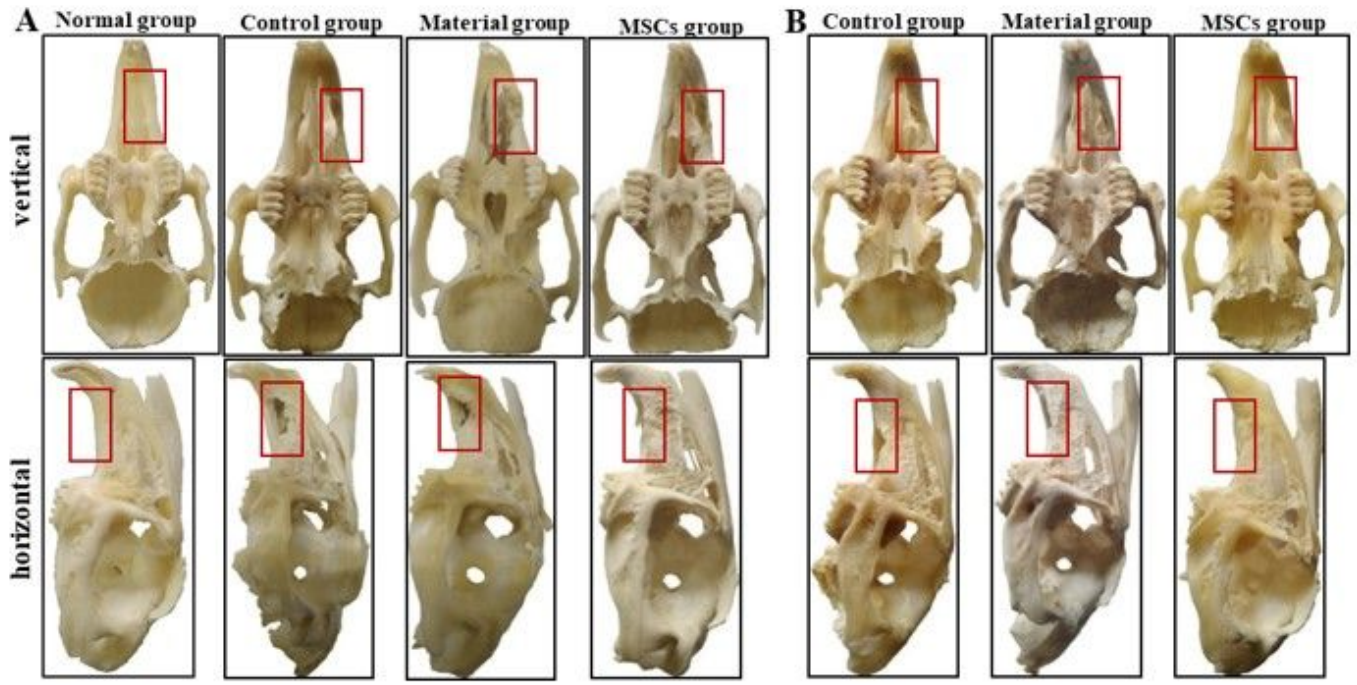

Figure 2

The general appearance of the skull. A the general appearance of the skull 3 months after surgery; B the general appearance of the skull 6 months after surgery. The red box shows the postoperative appearance of the transplanted area.

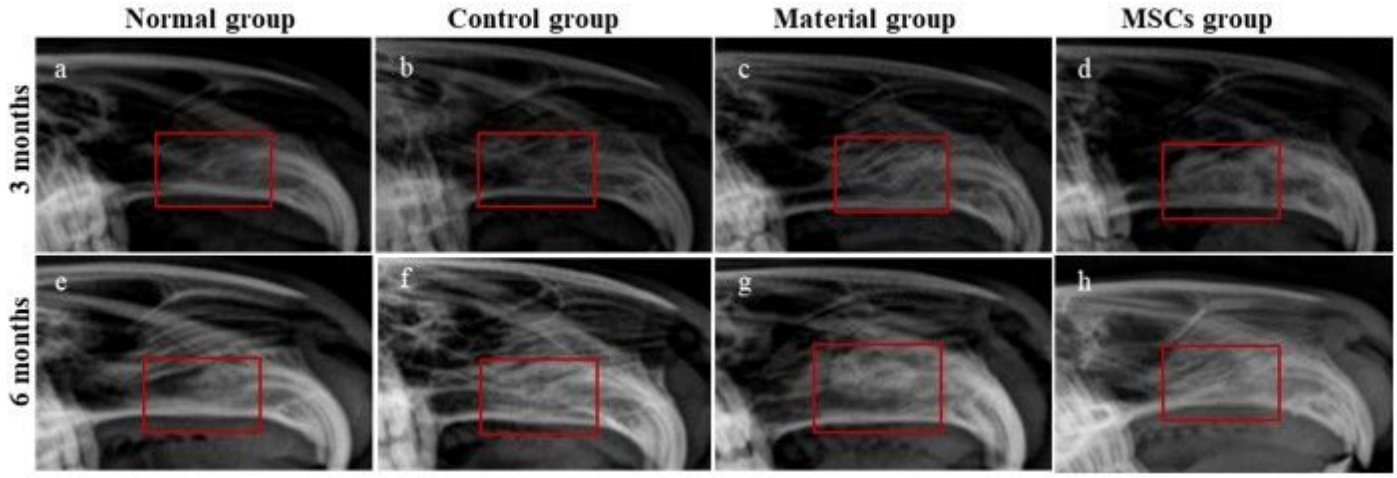

Figure 3

X-ray analysis results. a-d X-ray analysis of the skull 3 months after surgery; e-h X-ray analysis of the skull 6 months after surgery. a, e Normal group; b, f Control group; c, g Material group; d, h MSCs group. The

red box is the surgical area.

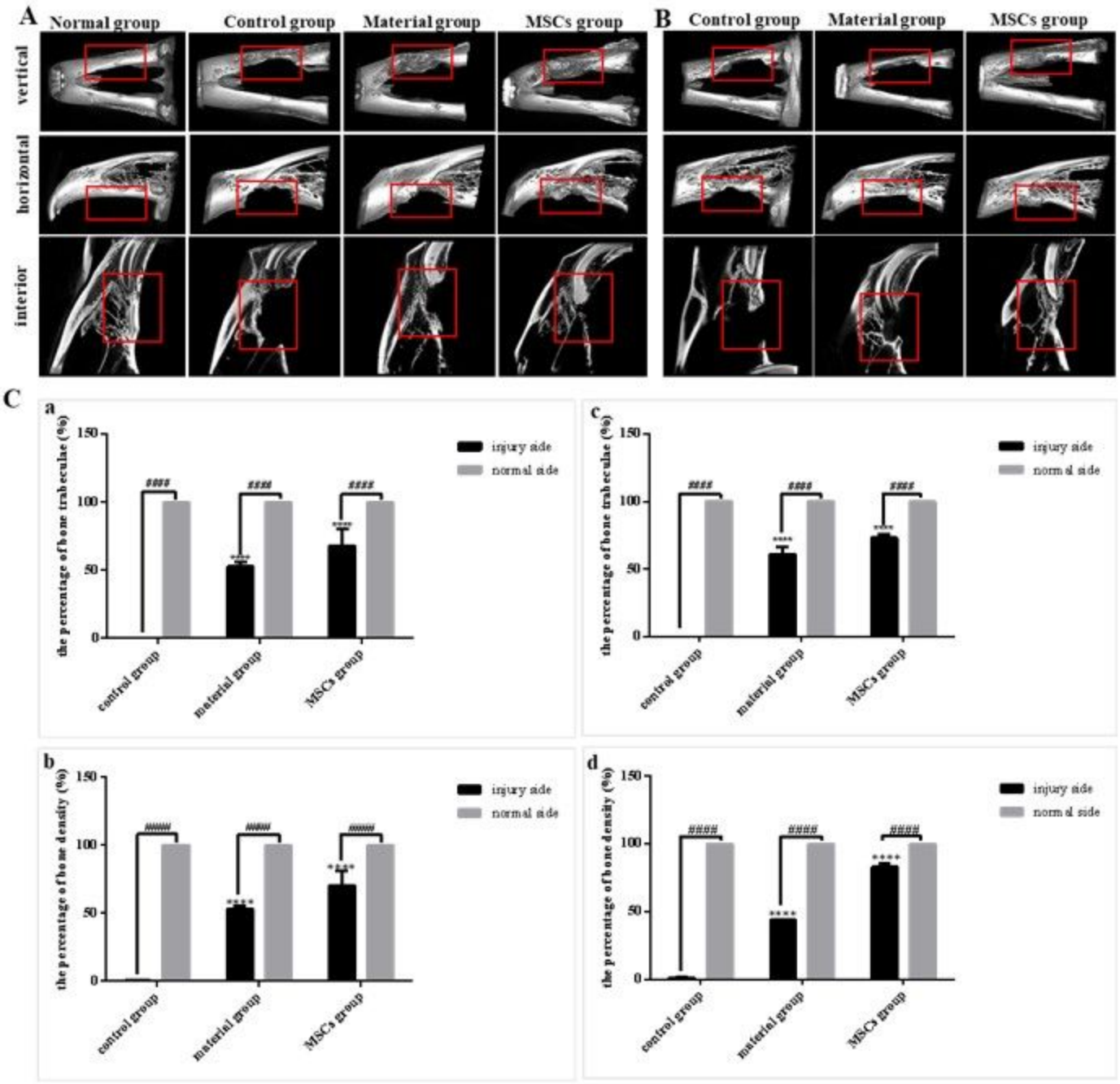

Figure 4

Micro CT results. A CT images from different angles 3 months after surgery; B CT images from different angles 6 months after surgery; C-a The percentage of bone trabeculae 3 months after surgery; C-b The percentage of bone density 3 months after surgery; C-c The percentage of bone trabeculae 6 months after; C-d The percentage of bone density 6 months after surgery. The injury side of each group was compared with that of the control group and the difference was denoted by *. The difference between the injury side and the normal side was expressed as #. #### , **** P□0.0001. The red box is the surgical area.

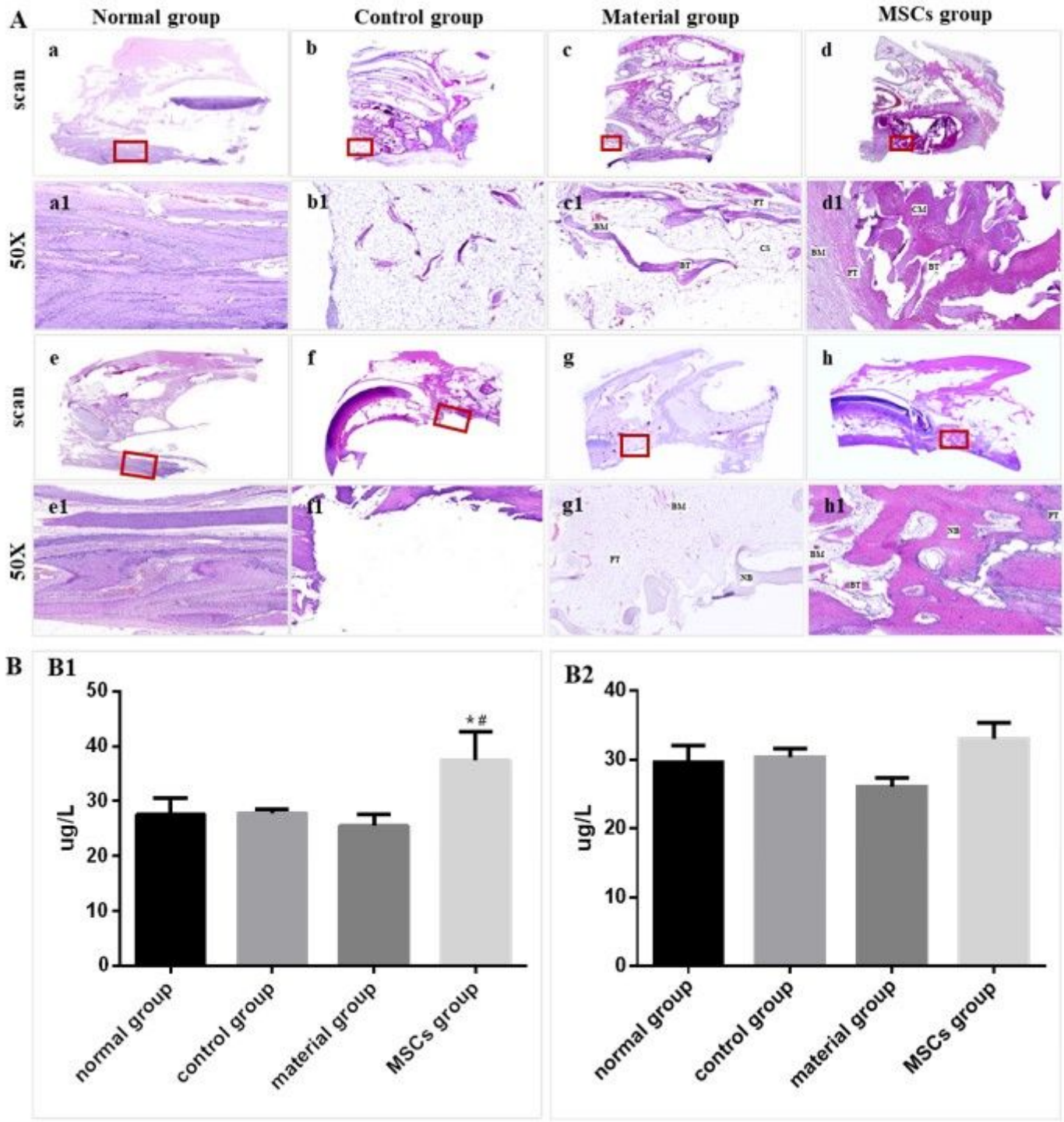

Figure 5

A HE staining results. B1 Serum BGP levels 3 months after surgery; B2 Serum BGP levels 6 months after surgery. The injury side of each group was compared with that of the control group and the difference was denoted by *. The difference between the injury side and the normal side was expressed as #. # , * P 0.05. a-d & a1-d1 HE staining results 3 months after surgery; e-h & e1-h1 HE staining 6 months after surgery. a, e & a1, e1 Normal group b, f & b1, f1 Control group c, g & c1, g1 Material group d, h & d1, h1 MSCs group. a-h The scan results of HE staining. a1-h1 The result of HE staining after 50 times

magnification. BM: bone marrow; FT: fibrous tissue; BT: bone trabecula; CM: collagen materials; NB: new bone; CS: cavitation structure.

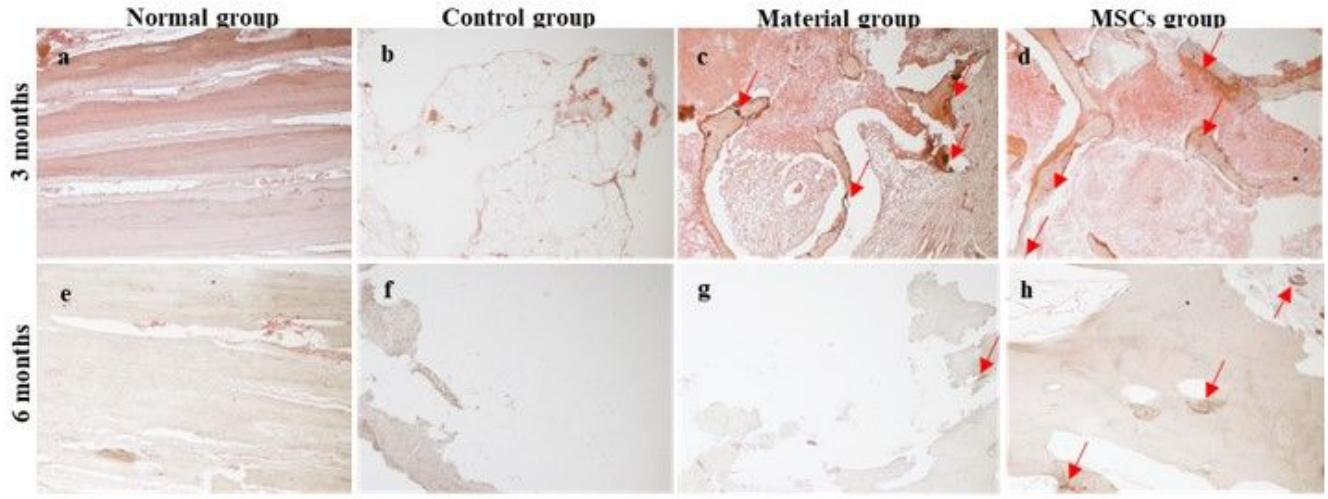

Figure 6

ALP staining results (100×). a-d ALP staining results 3 months after surgery; e-h ALP staining results 6 months after surgery. a, e Normal group; b, f Control group; c, g Material group; d, h MSCs group. Mark the area of the positive signal with a red arrow.

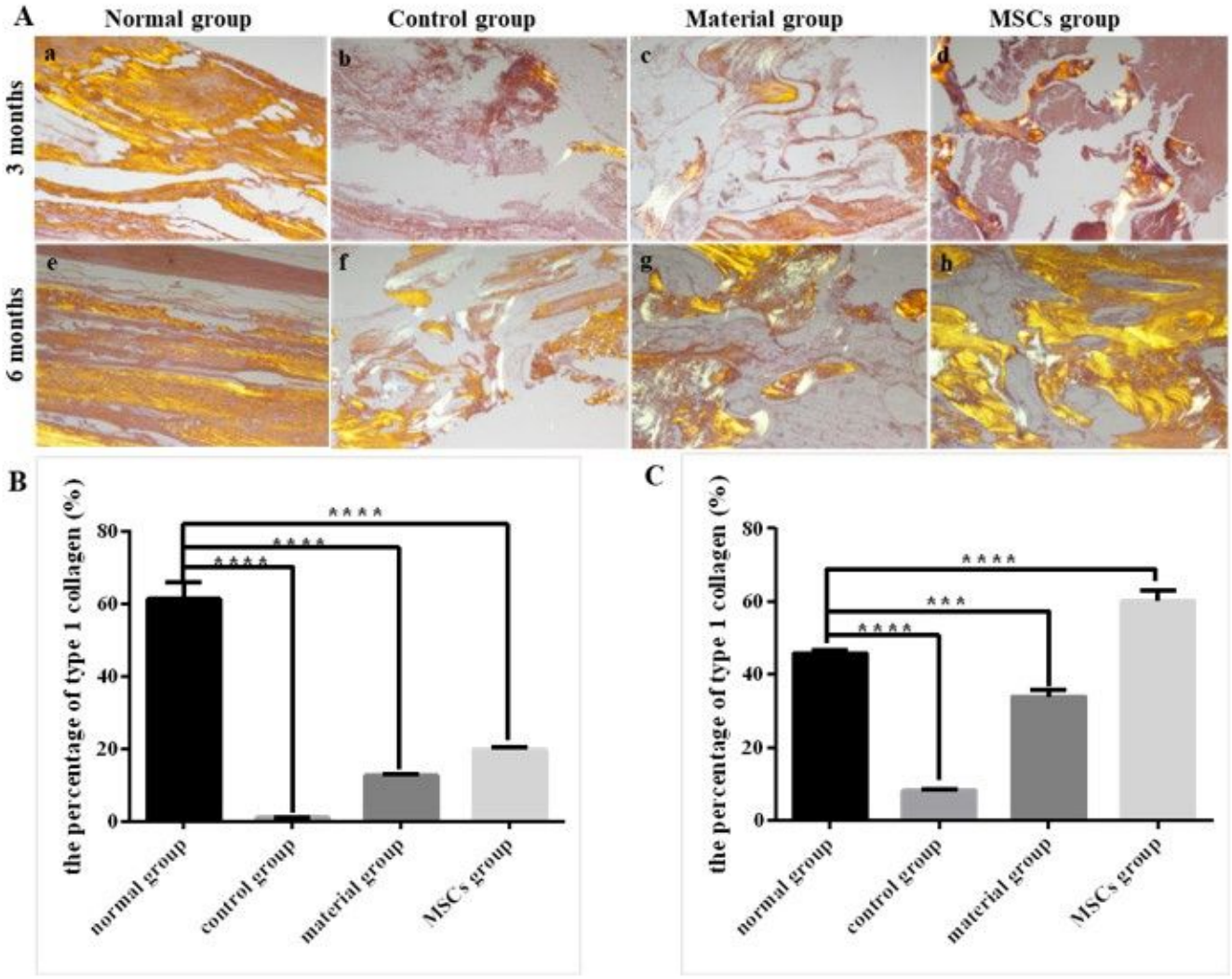

Figure 7

Sirius red staining results (40×). A a-d Sirius red staining results 3 months after surgery; e-h Sirius red staining results 6 months after surgery. a, e Normal group; b, f Control group; c, g Material group; d, h MSCs group. Mark the area of the positive signal with a red arrow. B The percentage of type 1 collagen 3 months after surgery. C The percentage of type 1 collagen 6 months after surgery. All groups were compared with the Normal group, and the statistical difference was denoted by *. *** P 0.001 ,**** P 0.0001.

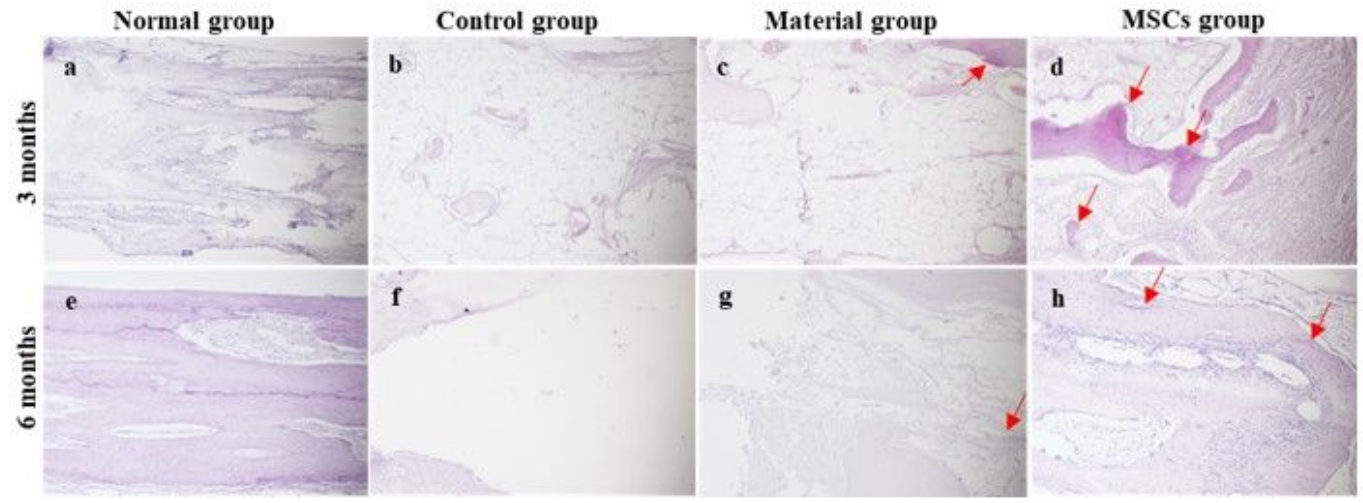

Figure 8

PAS staining results (100×). a-d PAS staining results 3 months after surgery; e-h PAS staining results 6 months after surgery. a, e Normal group; b, f Control group; c, g Material group; d, h MSCs group. Mark the area of the positive signal with a red arrow.

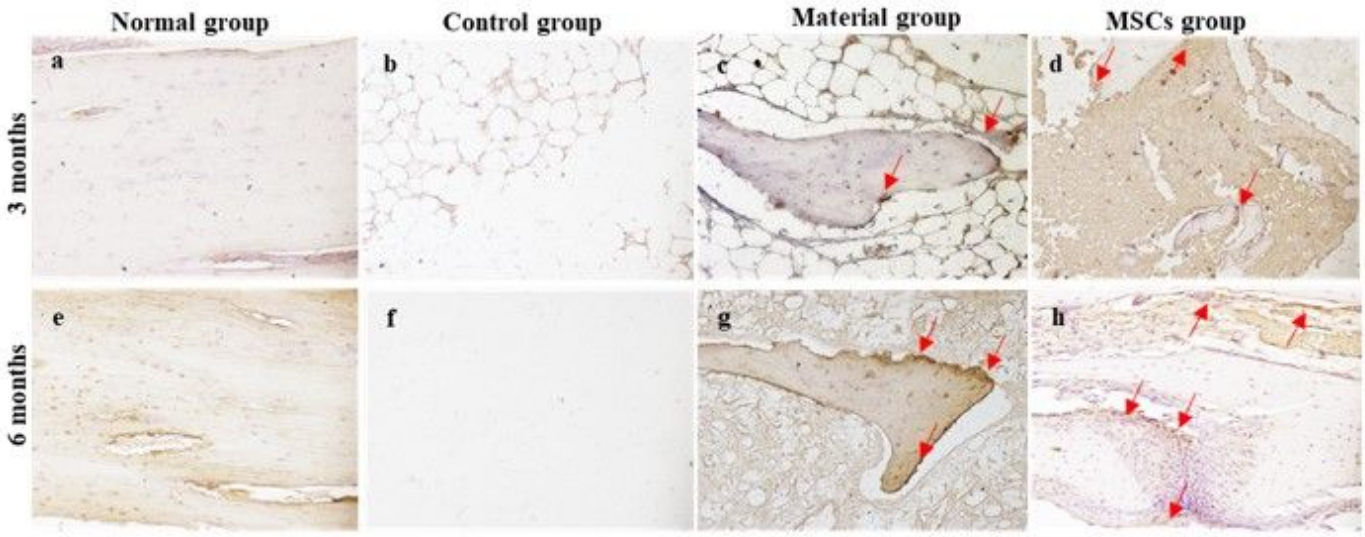

Figure 9

IHC results of BMP-2 (200×) a-d IHC results of BMP-2 3 months after surgery; e-h IHC results of BMP-2 6 months after surgery. a, e Normal group; b, f Control group; c, g Material group; d, h MSCs group. Mark the area of the positive signal with a red arrow.

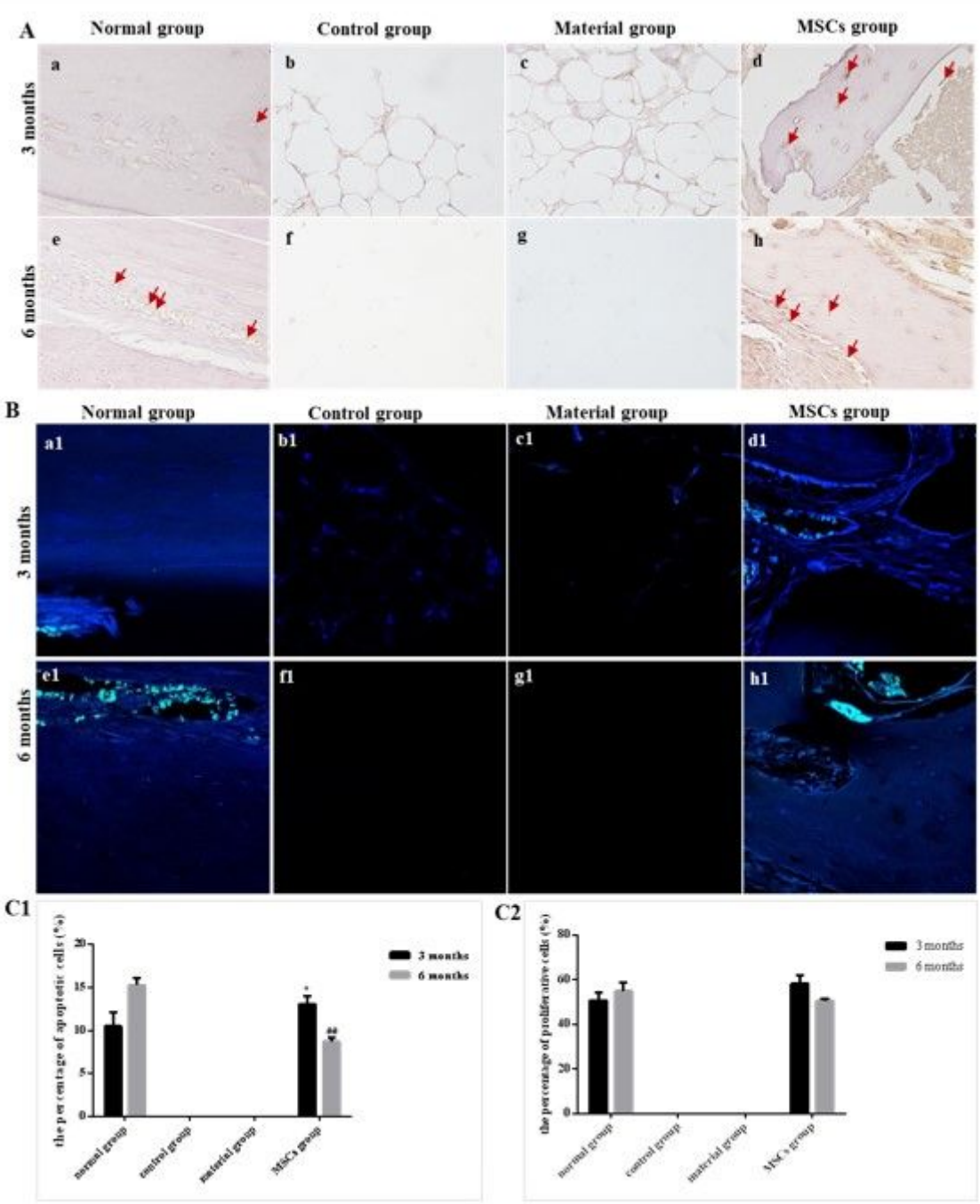

Figure 10

A TUNEL results (400×). B Ki67 results (400×). a-d & a1-d1 Results 3 months after surgery; e-h&e1-h1 Results 6 months after surgery. a, e & a1, e1 Normal group; b, f & b1, f1 Control group; c, g&c1,g1 Material group; d, h&d1,h1 MSCs group. C1 The percentage of apoptotic cells in each group at 3 or 6 months. C2 The percentage of proliferative cells in each group at 3 or 6 months. Cells labeled in green represent cells that are proliferating. * Represents the statistical difference between each group and the normal group. # represents the statistical difference between each group and the normal group. * $P < 0.05$; # # $P < 0.01$.